Electro-optical detection based on large Kerr effect in polymer-stabilized liquid crystals

Ru-Long Jin,[1] Yan-Hao Yu,[1] Han Yang,[1,3] Feng Zhu,[1] Qi-Dai Chen,[1] Mao-Bin Yi,[1] and Hong-Bo Sun[1,2,4]

[1]*State Key Laboratory on Integrated Optoelectronics, College of Electronic Science and Engineering, Jilin University, 2699 Qianjin Street, Changchun 130012, China*

[2]*College of Physics, Jilin University, 119 Jiefang Road, Changchun 130023, China*

[3]*e-mail: yanghan@jlu.edu.cn*

[4]*e-mail: hbsun@jlu.edu.cn*

Received November 28, 2011; accepted December 14, 2011;
posted January 11, 2012 (Doc. ID 159010); published February 22, 2012

In this Letter, polymer-stabilized liquid crystals with experimentally observed large electro-optic effect are introduced to the electro-optical detection to improve the voltage sensitivity. The Kerr constant of materials prepared in this study reached as high as 7.2×10^{-9} m/V^2, increasing by 1000 times the sensitivity of the conventional electro-optical materials. The noncontact detection configuration, using a laser beam as a probe, enables quick two-dimensional scanning measurements. © 2012 Optical Society of America

OCIS codes: 120.1880, 190.3270, 160.3710.

Electro-optical detection has proved to be a unique technique of increasing interest, which enabled many advances in electric field sensing, such as negligible perturbation and high spatial and temporal resolution [1,2]. One of the most important applications is detecting the local voltages on the transmission lines or nodes of integrated circuits (ICs) [3,4]. In this technique, an electro-optical material is sent into the fringing field of the IC surface, where its refractive indices vary with the applied field strength. The surrounding optical system converts the refractive index shifts into the detectable optical intensity modulation signals by polarizer or interference. As a result, the electric field information is acquired conveniently by detecting the probing beam intensity. However, the intrinsic low voltage sensitivity hampers the practical applications of electro-optical detection, because electro-optic coefficients of most known electro-optical materials are very small (usually only several pm/V) [2].

In recent decades many efforts have been devoted to improve the electro-optic behavior of engineered materials, such as new organic crystals [5] and poled polymers [6–8]. Therein, the potentially ultralarge electro-optic activity of polymer-stabilized liquid crystals (PSLCs) is quite attractive for electro-optical detection to enhance the voltage sensitivity [9–12]. The electro-optic Kerr constants of PSLCs were reported to be about a few 10^{-9} m/V^2, which are approximately 1000 times larger than those of conventional materials. Besides, the ease of material preparation with no need of high-temperature poling or complicated crystal growth process is another advantage. Here, these novel materials are introduced to the electro-optical detection, which exhibits a promising prospect to break through the sensitivity limit. Furthermore, the designed electro-optical probe configuration enables voltage-calibrated two-dimensional scanning measurement of local voltages of the IC surface.

The liquid-crystal materials used in this study consisted of a nematic mixture (60 wt% of WTK83100, HCCH, China) and 4-cyano-4'-pentylbiphenyl (40 wt% of 5CB). To prepare PSLCs, trimethylolpropane triacrylate (TMPTA) and phthalic diglycol diacrylate (PDDA) were used as monomers, and 2-hydroxy-2-methyl-1-propiophenone (darocure 1173) was used as a photoinitiator. To get a high electro-optic Kerr constant, chiral dopants (R1011 and CB15) of different weight ratios were added to the liquid-crystal host to tune the pitch of the given material, p. Each mixture (95% of liquid crystal and 5% of polymer) was sandwiched between two indium-tin-oxide (ITO) glass substrates with a cell gap of about 8 μm and followed by irradiation with ultraviolet light (UV) with an intensity of about 1 mW/cm^2 for 30 min at the temperature above the clear point.

Figure 1(a) shows the schematic experimental setup for measuring the field-induced birefringence of PSLCs. The PSLC cells are placed between the orthogonal polarizers and at an angle of 45° with respect to the incident light. The transmitted light intensity, which depends on the phase difference created by an electric field across

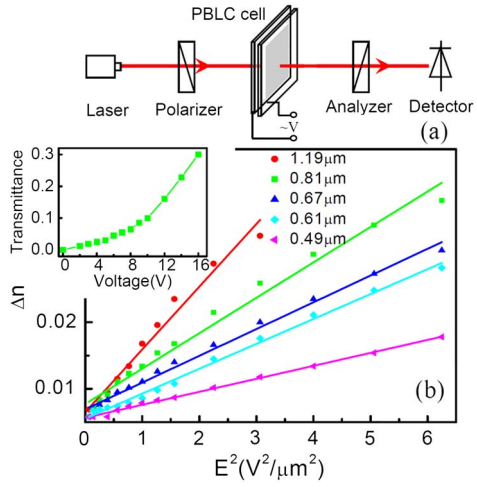

Fig. 1. (Color online) The field-induced birefringence measurement of PSLCs. (a) The schematic experimental setup. (b) The voltage-birefringence curves for the samples with different chiral pitches. The inset shows the voltage-transmittance curves of PSLCs of 0.81 μm pitch.

the sample, is detected by a photodiode. The observed output intensity, I_{out}, is expressed by

$$I_{out} = I_{in} \sin^2(\pi L \Delta n/\lambda), \quad (1)$$

where I_{in} is the input intensity, L is the light path length in PSLCs, Δn is the electric-induced birefringence, and λ is the wavelength of the probing beam. Thus, the electric-induced birefringence (Δn) can be evaluated from the ratio of transmitted light intensity. The inset of Fig. 1(b) shows the voltage-transmittance (V-T) curves of PSLCs of 0.81 μm pitch. For PSLCs, Δn is caused by the Kerr electro-optic effect, which is defined by

$$\Delta n = \lambda K E^2, \quad (2)$$

where K is the Kerr constant and E is the applied field strength. The voltage-birefringence (V-B) curves of liquid-crystal materials with different chiral pitches were presented in Fig. 2. It indicates that the Kerr constant decreases with the reduction of the chiral pitch [13]. Calculated from the slopes of the V-B curves, the highest Kerr constant of those materials (1.19 μm pitch) reached as large as about 7.2×10^{-9} m/V^2. These cholesteric liquid crystals show focal conic texture. This texture has high light scattering owing to the mismatch of the refractive index of different domains. In electro-optical measurement, the field-induced reorientation of liquid-crystal molecules will result in different scattering to the probing beam, which further enhances the voltage sensitivity. However, longer helical pitches increase instability in materials where the focal conic texture is easily converted to the planar texture. Therefore, with a reasonable compromise, we chose PSLCs of 1.19 μm pitch as a field-sensing material in electro-optical detection.

Figure 2 shows the schematic electro-optical system based on PSLC and the probe configuration (the inset) [14,15]. Unlike conventional external probes where the electro-optical material is attached to the tip end of a glass cone or a fiber, PSLC materials before UV curing are directly pasted upon the circuit under test. This detection means offers several advantages: (1) it uses the focused laser beam as a probe, which overcomes the complexity of the precision positioning of conventional external probes [16]; (2) because of the fluidity of PSLC materials before curing, field-sensing materials could tightly couple with the circuit surface; and (3) an ITO layer is introduced to screen all the fringing electric field of the given circuit in the PSLCs. As seen in probe configuration, one beam, reflected by the ITO interface, is called the reference beam (I_{ref}), and the other one, traveling through the PSLC layer and reflected by the measurement point, is called the probing beam (I_{pro}). Because of the Kerr effect of PSLCs, the information of the electric signals is converted to the detectable optical intensity signals by the interference of these two beams. The modulation signals are followed by electrical amplifying and then are sent to a monitoring computer. According to the mechanism mentioned above, the electric signals of the measurement points could be deduced from the modulation signals to achieve the purposes of the electro-optical detection.

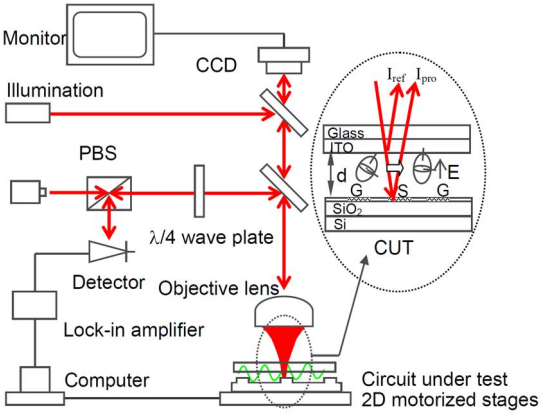

Fig. 2. (Color online) The schematic electro-optical system based on PBLCs. The inset shows the probe configuration.

In our experiments, the coplanar waveguides fabricated by photolithography were used to serve as circuits under test as seen in the inset of Fig. 3. The lines of the coplanar waveguides correspond to the transmission lines on the circuit surface. The light spot on the lines (the inset of Fig. 3) is the focused spot of the probe beam, the measurement point. The PSLC material of 1.19 μm pitch was selected because of its large Kerr coefficient. Figure 3 is the typical data picked up in the computer, which shows the modulation signal as a function of time when a square wave of 4 V was applied to the line of the coplanar waveguide. Because of the Kerr constant of several 10^{-9} m/V^2, the voltage sensitivity was enhanced by nearly 1000 times more than that of conventional materials. It greatly helps alleviate the stress of the electrical amplifier in the electro-optical system (Fig. 2). The challenges associated with the amplifier of high power gain, board bandwidth, and low noise are used to limit the practical application of the electro-optical detection. The response time is another important parameter for electro-optical detection. The rising time was measured to be 0.45 ms and the falling time was 0.55 ms. Different from crystal materials or poled polymers, the electro-optic effect of PSLCs originates from the field-induced molecular reorientation so that the response speed is relatively slow. Although ICs often operate at high frequency (GHz), this submillisecond technique is of value to the quasi-static detection for IC diagnosis to eliminate the influence of high-frequency parasitic parameter [17].

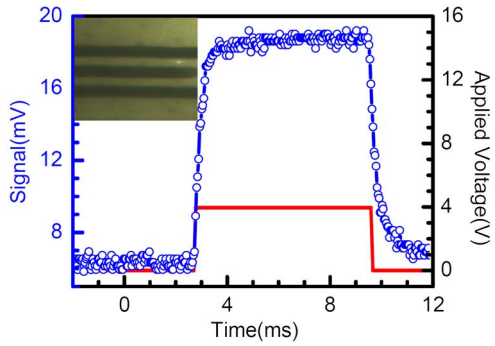

Fig. 3. (Color online) The typical data of the electro-optical probe experiment. The solid line is the applied electric signal to the line of the coplanar waveguide, and the circle-dot line shows the modulation light intensity read by a photodiode detector. The inset is the measured circuit and the spot of the probing beam monitored by a camera.

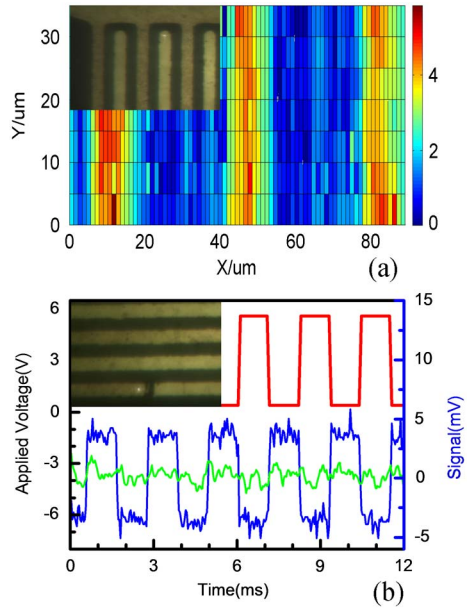

Fig. 4. (Color online) The electro-optical measurement of interdigital electrodes. (a) The measured two-dimensional electric distribution. (b) The measurement of an electrode with open defects. The upper curve is the applied voltage, and the lower curves are the signals measured on each side of the broken line. The insets of (a) and (b) are the interdigital electrodes with their finger and spacing of 10 μm.

As seen in Fig. 3, the PSLCs exhibit hysteresis that signal intensity did not return to the original level when the applied voltage was turned off. However, the signals we detected on the IC lines or nodes are usually continuous alternating signals but not direct current (DC) signals. The field-induced reorientation of PSLCs is in dynamic balance. Therefore, hysteresis will not give rise to large influence in electro-optical detection. If we detect a DC signal, extension of the measurement time would be a method to solve this problem.

In the process of electro-optical detection based on PSLCs, the sensing structure does not exist independently as a probe but attaches to the circuit under test. Therefore, the probe beam gets liberated from the substrate (a glass cone or a fiber as a waveguide) of the conventional external probe. It enables quick two-dimensional scanning measurements without complicated probe-location equipment. As seen in Fig. 2, a computer-controlled precision two-dimensional stage was equipped under the circuit. The spatial resolution is determined by the minimum focused spot size of the probing beam. According to the theory of diffraction, the spot diameter of Gauss beam is expressed as

$$d = \frac{2\lambda\sqrt{1 - \mathrm{NA}^2}}{\pi \mathrm{NA}}, \tag{3}$$

where λ is the wavelength of the probing beam and NA is the numerical aperture of the objective lens. Here $\lambda = 1.31$ μm, NA $= 0.55$, so the theoretical limit of the light spot is about 1.25 μm. An interdigital electrode with its finger and spacing of 10 μm was designed for the electro-optical detection of high spatial resolution [the inset of Fig. 4(a)]. The circuit was scanned by 1.25 μm per step horizontally and 5 μm per step vertically.

Figure 4(a) shows the two-dimensional electric distribution in the electrode with a voltage calibration method in Ref. 18. The measurement result was well in agreement with the theoretical expectations: the voltage on the signal line is 4 V and that on the ground line or the spacing is 0 V. A faulty electrode as the inset of Fig. 4(b) was presented to imitate a circuit with open defects. As predicted, the modulation signal was detected on one side of the broken line, but on the other one, no birefringence was induced [Fig. 4(b)]. Therefore, such detection satisfies the demand for IC fault diagnosis, particularly the physical defects, i.e., bridging shorts, gate oxide defects, and open defects [17].

In summary, employing PSLC materials with experimentally observed large Kerr constants, an electro-optical detection system was investigated. On the one hand, the excellent electro-optic activity enhanced the voltage sensitivity by about 1000 times. On the other hand, the novel probe configuration facilitates quick two-dimensional scanning measurements with micron class resolution. By the measurement of a faulty electrode, the capability for IC detection of this technique was confirmed.

The work is supported by the Natural Science Foundation of China under Grants No. 90923037 and No. 61077002.

References

1. Q. Wu and X. C. Zhang, Appl. Phys. Lett. **68**, 1604 (1996).
2. O. Mitrofanov, A. Gasparyan, L. N. Pfeiffer, and K. W. West, Appl. Phys. Lett. **86**, 202103 (2005).
3. M. Shinagawa and T. Nagatsuma, IEEE Trans. Instrum. Meas. **41**, 375 (1992).
4. K. Yang, G. David, S. V. Robertson, J. F. Whitaker, and L. P. B. Katehi, IEEE Trans. Microwave Theory Tech. **46**, 2338 (1998).
5. P. Y. Han, M. Tani, F. Pan, and X. C. Zhang, Opt. Lett. **25**, 675 (2000).
6. T. D. Kim, J. Luo, J. W. Ka, S. Hau, Y. Tian, Z. Shi, N. M. Tucker, S. H. Jang, J. W. Kang, and A. K.-Y. Ken, Adv. Mater. **18**, 3038 (2006).
7. H. Y. Woo, H. K. Shim, and K. S. Lee, Macromol. Chem. Phys. **199**, 1427 (1998).
8. K. Ariga, J. P. Hill, and Q. Ji, Phys. Chem. Chem. Phys. **9**, 2319 (2007).
9. Y. Haseba, H. Kikuchi, T. Nagamura, and T. Kajiyama, Adv. Mater. **17**, 2311 (2005).
10. Y. C. Yang and D. K. Yang, Appl. Phys. Lett. **98**, 023502 (2011).
11. S. Acharya, S. Kundu, J. P. Hill, G. J. Richards, and K. Ariga, Adv. Mater. **21**, 989 (2009).
12. S. Kundu, J. P. Hill, G. J. Richards, K. Ariga, A. H. Khan, U. Thupakula, and S. Acharya, ACS Appl. Mater. Interfaces **2**, 2759 (2010).
13. H. Choi, H. Higuchi, and H. Kikuchi, Appl. Phys. Lett. **98**, 131905 (2011).
14. R. L. Jin, H. Yang, D. Zhao, Q. D. Chen, Z. X. Yan, M. B. Yi, and H. B. Sun, Opt. Lett. **35**, 580 (2010).
15. R. L. Jin, H. Yang, Y. H. Yu, D. Zhao, J. Yao, F. Zhu, Q. D. Chen, M. B. Yi, and H. B. Sun, Opt. Lett. **36**, 1158 (2011).
16. T. Nagatsuma, T. Shibata, E. Sano, and A. Iwata, J. Appl. Phys. **66**, 4001 (1989).
17. R. Rajsuman, Proc. IEEE, **88**, 544 (2000).
18. R. L. Jin, H. Yang, D. Zhao, F. Zhu, Y. H. Yu, Q. D. Chen, M. B. Yi, and H. B. Sun, J. Photon. **1**, 57 (2011).